

Spectral functions in itinerant electron systems with geometrical frustration

Yoshiki Imai and Norio Kawakami

Department of Applied Physics, Osaka University, Suita, Osaka 565-0871, Japan

(Received 22 December 2001; published 28 May 2002)

The Hubbard model with geometrical frustration is investigated in a metallic phase close to half-filling. We calculate the single particle spectral function for the triangular lattice within dynamical cluster approximation, which is further combined with noncrossing approximation and fluctuation exchange approximation to treat the resulting cluster Anderson model. It is shown that frustration due to nonlocal correlations suppresses short-range antiferromagnetic fluctuations and thereby assists the formation of heavy quasiparticles near half-filling.

DOI: 10.1103/PhysRevB.65.233103

PACS number(s): 71.10.Fd, 71.27.+a

Recently, geometrically frustrated metallic systems have attracted much attention, for which a wide variety of interesting phenomena have been discovered. For instance, the compound LiV_2O_4 with pyrochlore structure, which is given by a corner-sharing network of tetrahedra of V ions, exhibits a heavy fermion behavior.¹ Also, another pyrochlore compound $\text{Y}(\text{Sc})\text{Mn}_2$ (Ref. 2) shows a quantum spin-liquid behavior down to low temperatures. These interesting phenomena are considered to be closely related to geometrical frustration^{3–8} induced by the strong Coulomb interaction with specific geometry of the lattice.

Among theoretical approaches to strongly correlated electron systems, dynamical mean field theory (DMFT) (Ref. 9) is one of the most successful methods to describe various physical properties. In DMFT the self-energy is given as a local quantity, which is justified in the limit of large dimensions.^{11,10} This method has been known as a good approximation even in three dimensions. However, since the self-energy becomes local in DMFT, nonlocal charge and spin correlations, which are essential for treating geometrical frustration, cannot be properly described in this framework. In order to deal with such nonlocal correlations, various approaches beyond the DMFT have been proposed.^{12–16} Among others, the dynamical cluster approximation (DCA) (Refs. 17–21) may provide a systematic way to incorporate nonlocal correlations. In DCA, the lattice problem is replaced by the corresponding cluster one embedded in an effective medium determined self-consistently. This method has the following nice features: the algorithm is fully causal and the approximation can be improved systematically if the cluster size is increased.

In this paper, we investigate the effects of geometrical frustration on the Hubbard model. In particular, we focus on the triangular lattice, which is known as a prototypical system having strong geometrical frustration. Since it is important to incorporate short-range correlations systematically, we employ DCA, which is further combined with noncrossing approximation (NCA) (Refs. 22,23) to solve the local problem. We also use a weak-coupling approach by means of fluctuation exchange approximation (FLEX) (Ref. 24) for the local problem, which should be complementary to the treatment of NCA. By calculating the one-particle spectral function as well as the total density of states in these approximations, we discuss how geometrical frustration effects the formation of heavy quasiparticles in a metallic phase close to half-filling.

We start with the single-band Hubbard model,

$$H = -t \sum_{\langle i,j \rangle \sigma} c_{i\sigma}^\dagger c_{j\sigma} - t' \sum_{\langle i,j' \rangle \sigma} c_{i\sigma}^\dagger c_{j'\sigma} + U \sum_i n_{i\uparrow} n_{i\downarrow}, \quad (1)$$

where $c_{i\sigma}$ ($c_{i\sigma}^\dagger$) is the annihilation (creation) operator of an electron with spin σ at the i th site, and U represents the Coulomb repulsion. We introduce two kinds of hopping parameters t and t' ($t' \leq t$) to study the effects of geometrical frustration systematically⁸ [Fig. 1(a)].

In order to apply DCA to the frustrated lattice system, we first introduce the N_c discrete cluster-momenta \mathbf{K} ,^{17–21} which are defined as

$$\mathbf{K} = n\mathbf{a}_1 + m\mathbf{a}_2, \quad (2)$$

$$\mathbf{a}_1 = \left(\frac{2\pi}{\sqrt{N_c}}, \frac{2\pi}{\sqrt{3N_c}} \right), \quad \mathbf{a}_2 = \left(0, \frac{4\pi}{\sqrt{3N_c}} \right), \quad (3)$$

where n and m denote the integral number and \mathbf{K} should be within the first Brillouin zone (BZ). Next, we divide the original BZ into the subregions specified by the cluster momenta (coarse-graining cells); an example of $N_c = 4$ is shown schematically in Fig. 1(b). Therefore, in our treatment the coarse-grained Green function,^{17–21}

$$\bar{G}_\sigma(\mathbf{K}, z) = \frac{1}{N'} \sum_{\tilde{\mathbf{k}}} \frac{1}{z - \epsilon_{\mathbf{K}+\tilde{\mathbf{k}}} - \Sigma_\sigma(\mathbf{K}, z)}, \quad (4)$$

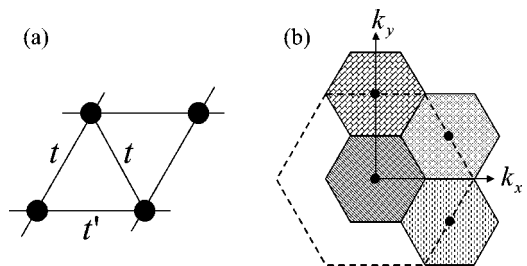


FIG. 1. (a) Schematic representation of triangular lattice with electron hoppings t and t' . (b) Example of the coarse-graining cells in the BZ for the triangular lattice, where the cluster size $N_c = 4$ and the dashed line denotes the first BZ. The dots represent the cluster momenta \mathbf{K} .

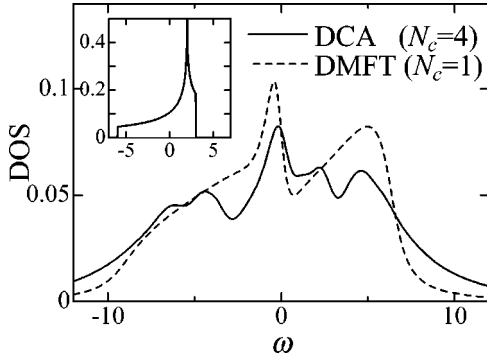


FIG. 2. Total DOS for the triangular lattice with DCA (solid line) and DMFT (dashed line) at half-filling, respectively. Here, the cluster size $N_c=4$. The energy is measured from the Fermi level ($\omega=0$). The parameters are chosen as $t'=t$, $U=6.0$, and the temperature $T=0.6$ (t is taken as the unit of the energy). The inset shows DOS for the noninteracting tight-binding model on the same lattice.

is specified by the cluster momentum \mathbf{K} . Here, $N'=N/N_c$ where N is the number of total lattice sites. The summation over $\tilde{\mathbf{k}}$ is taken within the coarse-graining cell.

In order to obtain the coarse-grained Green function, we now map the Hubbard lattice model to the cluster Anderson model.¹⁹ By solving this effective cluster problem, we can obtain the cluster self-energy $\Sigma(\mathbf{K},z)$, so that the coarse-grained Green function is determined self-consistently. Then the one-particle spectral function and the total DOS are given by the standard formula,

$$A_\sigma(\mathbf{K},\omega) = -\frac{1}{\pi} \text{Im} \bar{G}_\sigma(\mathbf{K},\omega); \quad (5)$$

$$\rho_\sigma(\omega) = \frac{1}{N_c} \sum_{\mathbf{K}} A_\sigma(\mathbf{K},\omega). \quad (6)$$

We numerically iterate the above procedure until the calculated quantities converge within desired accuracy. In the following discussions, we shall deal with a paramagnetic metallic phase. We set $t=1$ as the unit of the energy for simplicity.

In order to solve the cluster problem mentioned above, we make use of NCA,¹⁹ which is expected to provide reliable results in the temperature range we are now interested in. Since the dimension of the cluster Hamiltonian is 4^{N_c} , so that the numerical calculation becomes much more difficult with the increase of the number of cluster momenta. We practically take the cluster size, $N_c=4$ within the NCA in this paper. Note that we have neglected off-diagonal terms in the cluster resolvents, since those are known to be less important for discussing the one-particle spectra.¹⁹ We show our results calculated for $T=0.6$ below, since this temperature is reasonably low for our system to exhibit essential properties due to the electron correlations.

Let us first discuss the total DOS in the system with strong frustration. In Fig. 2, we show the DOS for the triangular lattice at half-filling with isotropic hopping, $t'=t$. For

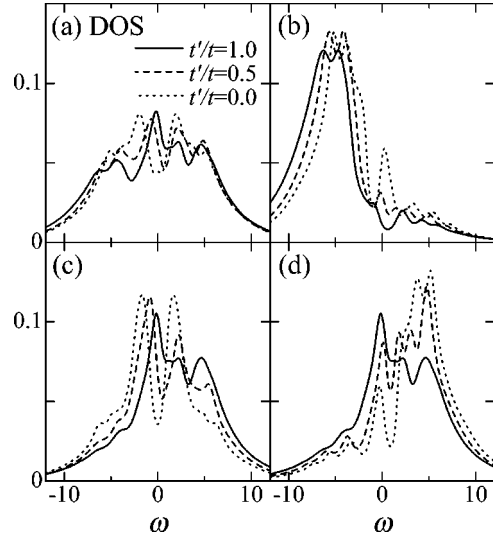


FIG. 3. (a) Total DOS $\rho(\omega)$ and (b)–(d) one-particle spectral functions $A(\mathbf{K},\omega)$ corresponding to the $\mathbf{K}=(0,0)$, $(\pi,\pi/\sqrt{3})$ [or $(\pi,-\pi/\sqrt{3})$] and $(0,2\pi/\sqrt{3})$ for various choices of the hopping amplitude: $t'=t$ (solid line), $t'=0.5t$ (dashed), and $t'=0.0$ (dotted). The other parameters are as in Fig. 2.

the triangular lattice, DOS calculated by DMFT has a many-body peak around the Fermi level ($\omega \sim 0$), which implies the formation of heavy quasiparticles due to the Hubbard interaction. We note here that the DCA recovers the DMFT for $N_c=1$. Even if short-range nonlocal correlations are taken into account by DCA, the many-body peak still persists although it becomes slightly smaller than that of DMFT.

This Fermi-liquid-like behavior is contrasted to the case of the square lattice with nearest neighbor hopping. In the latter case, it is known that a pseudo-gap structure in DOS, which is developed by the Hubbard interaction, prevents the formation of quasiparticles¹⁹ when the system is at half-filling where short-range antiferromagnetic fluctuations are most relevant (see also Fig. 3). Our results in the triangular lattice shows that antiferromagnetic correlations are strongly suppressed in the frustrated lattices, resulting in the formation of heavy quasiparticles even at half-filling. Note that in both of these two lattices, the Mott insulator is stabilized.

To investigate how antiferromagnetic fluctuations are suppressed by geometrical frustration, we change t' continuously, and observe what happens for the DOS and the one-particle spectral functions on the triangular lattice. The results are shown in Fig. 3. Note that the effect of frustration becomes less important with the decrease of t' . As t' decreases from t , the heavy quasi-particle band around the Fermi level is obscured, and then the pseudogap is developed after frustration is suppressed. From the one-particle spectral function for each momentum, shown in Figs. 3(b)–3(d), we can figure out which contribution is most relevant to the quasiparticle formation (or suppression) under strong frustration. Since the state with $\mathbf{K}=(0,0)$ is away from the Fermi level, the overall structure is not changed by t' . However the spectrum for $\mathbf{K}=(\pi,\pi/\sqrt{3})$, which is energetically degenerate with that for $\mathbf{K}=(\pi,-\pi/\sqrt{3})$, crosses the Fermi surface, being easily affected by frustration. When t' is equal to t ,

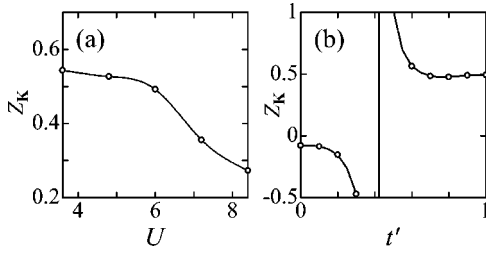


FIG. 4. Renormalization factor for the triangular lattice. (a) U -dependence ($t'=t$) and (b) t' -dependence ($U=6.0$). Here, $\mathbf{K}=(\pi, \pi/\sqrt{3})$. The other parameters are as in Fig. 2.

where frustration is very strong, heavy quasiparticles are formed around the Fermi level. With decreasing frustration, the heavy quasiparticle band splits, and the pseudogap begins to develop explicitly around the Fermi level. Therefore, the low energy physics in this system is mainly controlled by the state with $\mathbf{K}=(\pi, \pi/\sqrt{3})$ [or $\mathbf{K}=(\pi, -\pi/\sqrt{3})$].

In order to further confirm the above statements, we have numerically estimated the renormalization factor, which is defined as

$$Z_{\mathbf{K}} = \left(1 - \frac{\partial \Re \Sigma(\mathbf{K}, \omega)}{\partial \omega} \Big|_{\omega=0} \right)^{-1}. \quad (7)$$

In Fig. 4 we show the results obtained for the momentum $\mathbf{K}=(\pi, \pi/\sqrt{3})$ close to the Fermi level. It is seen from Fig. 4(a) that the renormalization factor for the triangular lattice is reduced with the increase of U for the fully frustrated case ($t'=t$). As mentioned above, this indicates that the effective mass near the Fermi level is enhanced by U , forming well-defined heavy quasiparticles. When t'/t is decreased from unity with U being fixed, the effect of frustration becomes less important, so that the system has a tendency to be an insulator with strong antiferromagnetic fluctuations. In this case, we encounter an anomalous behavior in the renormalization factor calculated numerically for the triangular lattice, as seen from Fig. 4. Namely, the renormalization factor increases as t' decreases, and diverges around $t'/t \sim 0.4$, below which it takes negative values. This anomalous behavior in $Z_{\mathbf{K}}$ is closely related to the formation of a dip-structure in the spectrum, which reflects the enhancement of antiferromagnetic fluctuations. The negative values of $Z_{\mathbf{K}}$ should be considered as an artifact of fitting the numerical data with the formula (7) even for the case with a dip structure.

So far, we have treated the effective cluster model by NCA, which may be an efficient approximation in the intermediate coupling regime. Here, we take a weak-coupling approach using FLEX to solve the effective cluster problem. Since FLEX is a perturbative method with respect to the Coulomb interaction U , it may give results complimentary to those of NCA. We here confirm the conclusion of the NCA approach by investigating effects of frustration on the triangular lattice in Fig. 1(a). Shown in Fig. 5 are the total DOS, the one-particle spectral function and the corresponding self-energy calculated for the triangular lattice at half-filling.

In the case of $t'=0$, a pseudogap develops around the Fermi level in the total DOS as well as in the one-particle

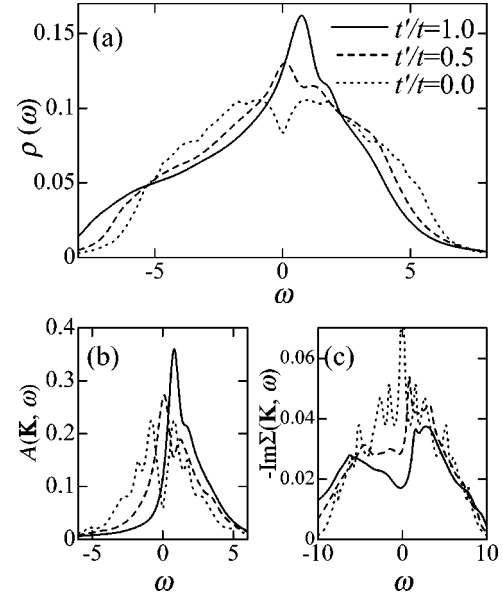


FIG. 5. (a) DOS $\rho(\omega)$, (b) one particle spectral function $A(\mathbf{K}, \omega)$ [$\mathbf{K}=(\pi, \pi/\sqrt{3})$], and (c) imaginary part of the self-energy $\Sigma(\mathbf{K}, \omega)$ for $U=3.0$, $T=0.6$ at half-filling. The cluster size N_c used for the calculation is 36.

spectral function as U increases, which is consistent with the QMC results^{20,21} and also with those obtained by NCA. It is seen that the pseudogap disappears with the increase of t' , similarly to the results of NCA. However, it is not clearly seen from this figure whether a heavy quasiparticle band is indeed formed, since the bump structure in the DOS above the Fermi level ($t'=0.5t$ and $1.0t$) is much effected by the van Hove singularity. Nevertheless, we can see a tendency to the formation of Fermi quasiparticles by observing the imaginary part of the self-energy in the large t' regime [Fig. 5(c)]. Namely, when t' is absent, the imaginary part of the self-energy has a sharp peak structure around $\omega \sim 0$, which is quite different from the Fermi-liquid behavior. However, with increasing t' , its shape changes from the peak to a concave structure, which is similar to a conventional Fermi liquidlike behavior. We have also checked that qualitatively analogous behaviors can be found in the system of different cluster size, $N_c=16$ and 64 . Therefore, we confirm the conclusion of the NCA approach that frustration assists the formation of Fermi quasiparticles by effectively suppressing the antiferromagnetic fluctuations.

We wish to mention here that our results are consistent with some experimental findings, e.g., the large specific-heat coefficient found in the pyrochlore compound, $\text{Y}(\text{Sc})\text{Mn}_2$,² which is a typical example of geometrically frustrated metallic systems.

In summary, we have investigated the Hubbard model with geometrical frustration by employing the triangular lattice as a typical example. Applying DCA combined with NCA and FLEX to the Hubbard model in a paramagnetic metallic phase close to the Mott insulator, we have calculated the one-particle spectral function. Based on the results obtained by both approaches, we have demonstrated how geo-

metrical frustration suppresses antiferromagnetic correlations, and then assists the formation of a heavy quasiparticle band near the Mott insulating phase.

We acknowledge valuable discussions with A. Koga and

A. Kawaguchi. The work is partly supported by a Grant-in-Aid from the Ministry of Education, Science, Sports, and Culture. Parts of the numerical computations were done by the supercomputer center at Institute for Solid State Physics, The University of Tokyo.

-
- ¹S. Kondo *et al.*, Phys. Rev. Lett. **78**, 3729 (1997).
²R. Ballou, E. Lelièvre-Berna, and B. Fåk, Phys. Rev. Lett. **76**, 2125 (1996).
³H. Kaps, N. Büttingen, W. Trinkl, A. Loidl, M. Klemm, and S. Horn, cond-mat/0004493 (unpublished).
⁴M. Isoda and S. Mori, J. Phys. Soc. Jpn. **69**, 1509 (2000).
⁵M. Capone, L. Capriotti, F. Becca, and S. Caprara, Phys. Rev. B **63**, 085104 (2001).
⁶M. D. Núñez-Regueiro and C. Lacroix, Phys. Rev. B **63**, 014417 (2001).
⁷S. Fujimoto, Phys. Rev. B **64**, 085102 (2001).
⁸T. Kashima and M. Imada, J. Phys. Soc. Jpn. **70**, 3052 (2001); H. Morita, S. Watanabe, and M. Imada, cond-mat/0203020 (unpublished).
⁹A. Georges, G. Kotliar, W. Krauth, and M. J. Rozenberg, Rev. Mod. Phys. **68**, 13 (1996).
¹⁰E. Müller-Hartmann, Z. Phys. B: Condens. Matter **74**, 507 (1989).
¹¹W. Metzner and D. Vollhardt, Phys. Rev. Lett. **62**, 324 (1989).
¹²P. G. J. van Dongen, Phys. Rev. B **50**, 14 016 (1994).
¹³A. Schiller and K. Ingersent, Phys. Rev. Lett. **75**, 113 (1995).
¹⁴Tran Minh-Tien, Phys. Rev. B **58**, 15 965 (1998).
¹⁵A. I. Lichtenstein and M. I. Katsnelson, Phys. Rev. B **62**, R9283 (2000).
¹⁶G. Kotliar, S. Y. Savrasov, G. Pálsson, and G. Biroli, Phys. Rev. Lett. **87**, 186401 (2001).
¹⁷M. H. Hettler, A. N. Tahvildar-Zadeh, M. Jarrell, T. Pruschke, and H. R. Krishnamurthy, Phys. Rev. B **58**, R7475 (1998).
¹⁸M. H. Hettler, M. Mukherjee, M. Jarrell, and H. R. Krishnamurthy, Phys. Rev. B **61**, 12 739 (2000).
¹⁹Th. Maier, M. Jarrell, Th. Pruschke, and J. Keller, Eur. Phys. J. B **13**, 613 (2000).
²⁰S. Moukouri and M. Jarrell, Phys. Rev. Lett. **87**, 167010 (2001).
²¹M. Jarrell, Th. Maier, C. Huscroft, and S. Moukouri, Phys. Rev. B **64**, 195130 (2001).
²²N. E. Bickers, Rev. Mod. Phys. **59**, 845 (1987).
²³Th. Pruschke and N. Grewe, Z. Phys. B: Condens. Matter **74**, 439 (1989).
²⁴N. E. Bickers, D. J. Scalapino, and S. R. White, Phys. Rev. Lett. **62**, 961 (1989).